

High Order Parametric Resonance and Nonlinear Mechanics of Nanowires: Techniques and Experiments

Min-Feng Yu* and Gregory J. Wagner**

*Department of Mechanical and Industrial Engineering, University of Illinois at Urbana-Champaign
1206 West Green Street, Urbana, IL, USA, mfyu@uiuc.edu

**Sandia National Laboratory, Livermore, CA, USA, gjwagne@sandia.gov

ABSTRACT

High order parametric resonances and mechanical studies in a nanowire mechanical system were realized using oscillating electric field induced oscillation. For the parametric resonance studies, resonance at drive frequencies near $2f_0/n$, where f_0 is the nanowire's fundamental resonance, for n from 1 to 4 were observed inside a scanning electron microscope, and analyzed. Such resonances were found to originate from the amplitude dependent electric field force acting on the nanowire and can be described by the Mathieu equation, which has known regions of instability in the parameter space. For the mechanical studies of nanowires, resonances of nanowires were used to deduce their elastic modulus and quality factor.

Keywords: nanowire, parametric resonance, nanomanipulation, mechanics, electron microscopy

1 INTRODUCTION

The extremely small physical dimensions of nanomaterials imply high sensitivity to external perturbation, which promises applications in sensing and micro-/nano- electromechanical systems [1, 2]. As one of the basic phenomena of any structure, mechanical resonance has been widely applied for studying the fundamental mechanics of nanoscale materials and utilized for making high sensitivity devices [3, 4].

For a freely-suspended, cantilevered simple beam, the equation of motion of the beam can be described by:

$$\rho A \frac{\partial^2 u}{\partial t^2} + EI \frac{\partial^4 u}{\partial x^4} = 0, \quad (1)$$

where u is the displacement, ρ is the density, A is the cross section area, E is the Young's modulus and I is the moment of inertial. The frequency ω_i of the i^{th} mode natural resonance is deduced from the equation:

$\omega_i = \beta_i^2 \sqrt{EI/\rho A} / L^2$, where β_i is the root of the boundary equation $\cos \beta_i \cosh \beta_i = -1$, and which is the basis of most techniques for measuring the Young's modulus of materials. An interesting phenomenon arises when a cantilevered beam is forced to a resonant oscillation. Parametric resonance describes such a resonance due to a

parametric excitation (a periodically varying coefficient) in the homogeneous equation of motion [5]. In a single-degree-of-freedom mechanical system, parametric resonance described by the Mathieu equation is:

$$\frac{d^2 Y}{dt^2} + \mu \frac{dY}{dt} + (a + 2\varepsilon \cos \omega t)Y = 0, \quad (2)$$

where Y is an angular or displacement variable, μ is the damping constant, and a and ε are system parameters. For an undamped system ($\mu = 0$), the theory predicts instabilities at $a = n^2/4$ for $n = 1, 2, \dots$, and regions of instability in parameter space described by a and ε . Such instabilities result in parametric resonances of the system at drive frequencies of $2\omega_0/n$, where ω_0 is the natural resonance frequency of the system. Though the realization of high order parametric mechanical resonance in macroscopic systems is generally difficult due to mechanical energy losses and strict conditions applied at higher n determined by the system parameters; high order (for n up to 4) parametric mechanical resonance was only recently observed in microscale MEMS resonators [4].

We report the application of resonance method for the study of mechanics of nanomaterials and the realization of up to four parametric resonances for cantilevered nanowires. A theory for describing the forced vibration that includes a forcing term proportional to the amplitude of the resonance was developed, regions of instability were mapped, and hysteresis in the parametric resonance response curve was observed.

2 EXPERIMENT

A four probe nanomanipulation tool (Fig. 1) with 12 degrees of freedom was developed for use inside a field emission scanning electron microscope (SEM) [6-8]. This tool is capable of nanometer resolution motion, and free-space manipulation/characterization of nanostructures by the four probes controlled by the precision manipulators. For the study of the resonance mechanics of nanowire, Fig. 2 shows the schematic of the experimental setup. A dc bias and an ac signal from a sine wave signal generator, which generates the oscillating electric field, are applied between the nanowire (attached on one electrode through manipulation) and a counter-electrode. By tuning the frequency of the ac signal, the cantilevered nanowire can be excited such that maximum amplitude is achieved when the

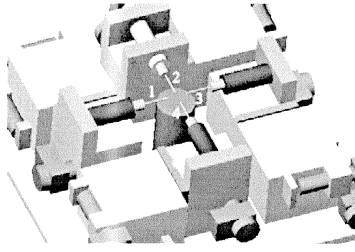


Fig. 1: Schematic of the multiple degrees of freedom nanomanipulation platform for use inside a scanning electron microscope.

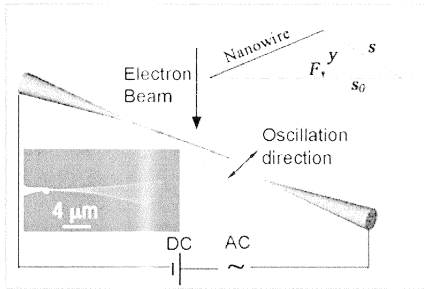


Fig. 2: Schematic of the experimental setup inside the SEM showing the resonating nanowire under the applied dc bias and ac drive signal. The top-right hand inset shows the geometric relation between the nanowire and the drive electrode along the plane of the nanowire vibration, the bottom-left hand inset shows a representative boron nanowire in resonance.

frequency of the drive signal matches the mechanical resonance frequency of the nanowire. We have successfully applied such a technique to induce the resonance of carbon and BN nanotubes, B and Si nanowires, and Ga_2O_3 nanowire and nanoribbon (Fig. 3). Quality factor as high as 3000 has been obtained from B nanowire resonator; and it falls between 100 and 600 for multiwalled carbon nanotube.

A computerized data acquisition system for acquiring the amplitude versus frequency response curve was developed. In the acquisition, the SEM beam control is set in line scan mode across the nanowire. The SEM line scan shows a narrow peak with a width roughly equal to the diameter of the nanowire when the nanowire is essentially stationary; it shows a broader plateau when the nanowire is driven into oscillation, and the width of the plateau corresponds to the amplitude envelope of the oscillation. The sine wave signal generator is programmed to tune the drive frequency at fixed step (1Hz to 10 kHz depending on the frequency resolution needed for the response curve), and at each step, the line scan signal is acquired and processed to obtain the amplitude of the driven nanowire at that driving frequency. Alternatively, by setting the beam control for the SEM in “spot mode” so that the beam scan is

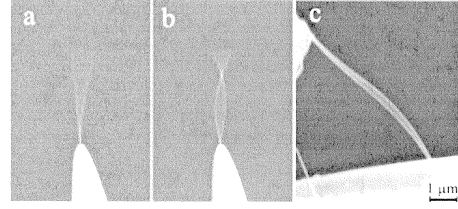


Fig. 3: Modes of resonant oscillations of cantilevered (a and b) and clamped (c) individual multiwalled carbon nanotubes.

stopped, a periodic signal from the SEM detector output can be acquired when the laterally resonating nanowire traverses the stationary electron beam. This technique provides a direct measurement of the real oscillating frequency and potentially phase of the nanowire.

3 THEORETICAL MODEL FOR THE FORCED OSCILLATION

The electric field-induced resonance of a cantilevered nanowire can be described as a nonlinear system with forced vibration. With a dc voltage V_{dc} and an ac drive signal $V_{ac}\cos(\Omega t)$, the forcing term $F(x, t)$ (where x is the distance along the nanowire) is $F(x, t) = -Q(x, t)V_{dc}^2 \left(1 + \beta^2/2 + 2\beta \cos \Omega t + \beta^2/2 \cos 2\Omega t \right)$, where $\beta = V_{ac}/V_{dc}$, the angular drive frequency Ω is related to f through $\Omega = 2\pi f$, and $Q(x, t)$ is a function that depends on the geometry and electrical parameters of the system. For small displacements of the nanowire, $Q(x, t)$ can be approximated by an expansion on $y(x, t)$ (the displacement of the nanowire): $Q(x, t) = Q_0(x) + Q_1(x)y(x, t) + O(y^2)$. The electric field force on a segment of the wire is a Coulomb force.

We include the effect of the electric field force to first order in y , and the equation of motion for the beam is:

$$\rho A \frac{\partial^2 y}{\partial t^2} + c \frac{\partial y}{\partial t} + EI \frac{\partial^4 y}{\partial x^4} = -V_{dc}^2 (1 + 2\beta \cos \Omega t) Q_1(x) y, \quad (3)$$

where ρ is the volume density ($2460 \text{ Kg}\cdot\text{m}^{-3}$ for boron), A is the cross sectional area, c is the damping coefficient, E is the bending modulus, and I is the area moment of inertia of the nanowire having a length L . Integrating over the beam length L to remove the x dependence gives an equation for the time dependence of each natural resonance mode:

$$\ddot{u}_i + \frac{c}{\rho A \Omega} \dot{u}_i + \frac{1}{\Omega^2} \left(\omega_i^2 + \frac{q_i V_{dc}^2}{\rho A \gamma_i} + \frac{2\beta q_i V_{dc}^2}{\rho A \gamma_i} \cos t \right) u_i = 0, \quad (4)$$

where $\omega_i = \kappa_i^2 \sqrt{EI/\rho A}$, $\gamma_i = L^{-1} \int_0^L \phi_i dx$, (note that ω_i is the natural angular frequency of mode i). Equation 4 has been made non-dimensional by scaling time with Ω^{-1} and length with L . This equation has the form of the damped

Mathieu equation (as described in Eq. 2), with parameters: $\mu = c/\rho A \Omega$, $a = \Omega^{-2}[\omega_i^2 + q_i V_{dc}^2/(\rho A \gamma_i)]$ and $\varepsilon = \Omega^{-2} \beta q_i V_{dc}^2/(\rho A \gamma_i)$. The vibration in our experiments is the fundamental mode ($i=0$) resonance, for which $\kappa_0 \approx 1.875/L$ and $\gamma_0 \approx 0.783$. Since the Mathieu equation has points of instability at values of a given by $n^2/4$, according to Eq. 4 this occurs for values of the driving frequency given by $\Omega_R = \frac{2}{n} \sqrt{\omega_0^2 + q_0 V_{dc}^2/(\rho A \gamma_0)}$. Note that these resonances are not exactly proportional to the natural frequency ω_0 , but instead are shifted by a small amount dependent upon q_0 and V_{dc} .

4 RESULTS AND DISCUSSIONS

Figure 4 shows the acquired amplitude-drive frequency curves of three parametric resonances centered at drive frequencies f of 0.453 MHz (close to $2f_0/3$), 0.674 MHz (the resonance frequency of the fundamental mode f_0) and 1.386 MHz (close to $2f_0$) for a boron nanowire [9] (The Young's modulus of the nanowire was estimated to be 230 GPa according to Eq. 1) as shown in the left hand inset in Fig. 4.

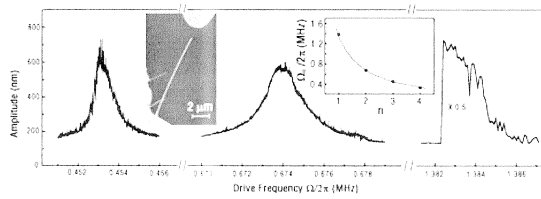


Figure 4: The amplitude versus drive frequency curves acquired at different V_{ac} and V_{dc} . The left hand inset shows the SEM image of the nanowire (11.6 μm long and 67 nm in diameter) and the drive probe tip (placed 1.5 μm away from the free end of the nanowire). The right hand inset shows the comparison between the drive resonance frequencies (square) obtained from the experiment and the curve according to the theory.

The resonance at $f = 0.329$ MHz (close to $f_0/2$) excited manually with $V_{dc} = 0$ V and $V_{ac} = 1$ V using another signal generator was also visually observed but the response curve was not acquired because the frequency was out of the range of the computer-controlled signal generator (0.4 MHz-1.1 GHz). A comparison between the experimental data (represented by solid squares in the plot) and the curve according to $\Omega_R = 2\omega_0/n$ is plotted in the right hand inset in Fig. 4, and shows an excellent agreement. The SEM spot mode method described above was used and found that the nanowire oscillated constantly near its fundamental frequency f_0 with the above four different drive frequencies, which is a characteristic of a parametric resonance system.

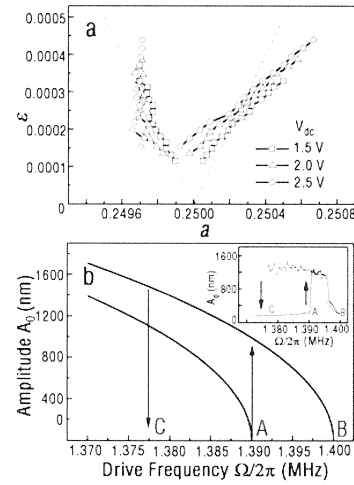


Figure 5: (a) Stability diagram for the parametric resonance $n=1$ of a boron nanowire having a diameter of 114 nm and a length of 10 μm . The dashed lines indicate the boundaries according to the theory. (b) Amplitude-frequency response curve obtained from modeling for the parametric resonance $n=1$ describes in Fig. 4. The arrowed lines indicate the locations of the possible jumps. The inset in (b) is the experimental result showing the hysteresis for the nanowire described in Fig. 4 acquired at $V_{dc} = 17.6$ V and $V_{ac} = 550$ mV.

Regions of mechanical instability in parameter space are expected as a result of the Mathieu equation. Figure 5a shows such a stability chart for a nanowire having a length of 10 μm and a diameter of 114 nm for its parametric resonance $n=1$. The plot was obtained by acquiring 42 amplitude versus frequency response curves at 42 pairs of V_{dc} and V_{ac} voltages. From each acquired response curve, two threshold frequencies, one at the jump up point such as the point A and another at the smoothly rising up point such as the point B in the response curve as shown in Fig. 5b, were determined. The jump down event such as at the point C in Fig. 5b is arbitrary depending on other high order perturbations in a large amplitude oscillation system, and is not related to the region of instability defined by the parametric resonance equation. The V_{dc} , V_{ac} and threshold frequencies were then converted to a and ε according to formulas derived in the paper, which resulted in the upper and lower boundaries for the instability region as shown in Fig. 5a. The plot clearly shows a “tongue” shape for the unstable region confined between the two linear boundaries as predicted by the Mathieu equation. The dashed lines in Fig. 5a are the predicted boundaries from the theory for comparison. Mapping the stability chart for higher-order parametric resonance, such as for $n = 3$, is difficult due to the higher excitation voltages needed for such mapping. Applying higher ac and dc voltage significantly disturbs the electron beam in the SEM imaging and thus the data acquisition.

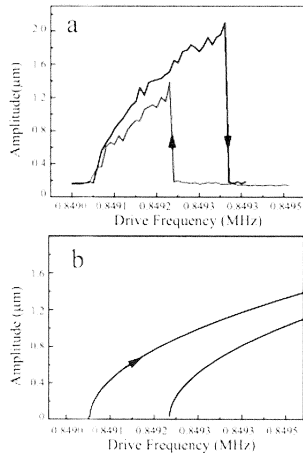


Fig. 6: Hysteresis in the amplitude versus drive frequency curve for a hardening nanowire mechanical system. (a) Experimental result; (b) the corresponding modeling result.

Hysteresis is seen from the frequency response curve for the parametric resonance $n=1$ of the nanowire at constant dc and ac bias as shown in the inset in Fig. 5b for a softening system and in Fig. 6a for a hardening system. Two curves acquired from a forward frequency sweep and from a backward frequency sweep are displayed. “Jump up” at point A and “jump down” at point C between the upper and lower branches of the response curve are clearly resolved, indicating that there is a portion of the response curve between points A and C that is unattainable.

This hysteresis can be understood by considering the nonlinear force-deflection behavior of the nanowire. In parametric resonance, unlike resonance of a simple mass-stiffness system, finite damping alone is not sufficient to keep the amplitude from growing to infinity as time increases; rather, the nonlinear behavior of the system must provide the upper limit to amplitude growth. To demonstrate this, we consider an undamped version of the Mathieu equation: $d^2u/dt^2 + (a + 2\epsilon \cos t)u \mp \epsilon au^3 = 0$, where α is assumed to give the relative size of a cubic nonlinearity in the system, and the negative sign is for a softening system and the positive sign for a hardening system. Using a multi-time expansion [10] in the small parameter ϵ , and considering values of the parameter a near 1/4 (so that $a=1/4+\epsilon a_1$), we derive periodic solutions having the form $u=A_0\cos(t/2+\theta)$. Three solutions for the steady-state amplitude exist for the softening mechanical system:

$A_0 = 0$, $A_0 = \frac{2}{\sqrt{3\alpha}}\sqrt{a_1 \pm 1}$. The presence of multiple stable solutions for $a_1 > -1$ explains the hysteresis seen in the experiment near $a=1/4$. For a hardening system,

$A_0 = 0$, $A_0 = \frac{2}{\sqrt{3\alpha}}\sqrt{-a_1 \pm 1}$. Fig. 5b and Fig. 6b shows the

response curve obtained according to these solutions obtained from such modeling.

A parametrically driven cantilevered nanowire can be designed to operate near the boundary conditions according to the stability chart, and could provide very effective response to either individual molecule or nanoparticle attachment by threshold transition for making “super-sensitive” sensors. A parametric resonator has also a unique feature that a normal resonator does not have. Parametric resonances only occur when the parameters lie in a *particular range*. For the case reported in this paper, three adjustable parameters define the stability chart: the ac and dc voltage and the frequency of the oscillating electric field.

ACKNOWLEDGMENT

MFY thanks the startup support from the University of Illinois. Contributions from and discussions with GJW, R. S. Ruoff, and M. J. Dyer are greatly appreciated.

REFERENCES

- [1] P. Poncharal, Z. L. Wang, D. Ugarte, and W. A. de Heer, *Science* **283**, 1513 (1999).
- [2] J. Kong, N. R. Franklin, C. Zhou, M. G. Chapline, S. Peng, K. Cho, and H. Dault, *Science* (Washington, D. C.) **287**, 622 (2000); T. W. Tombler, C. Zhou, L. Alexseyev, J. Kong, H. Dai, C. S. Jayanthi, M. Tang, and S.-Y. Wu, *Nature* (London) **405**, 769 (2000); Y. Cui, Q. Wei, H. Park, and C. M. Lieber, *Science* **293**, 1289 (2001); B. Ilic, D. Czaplewski, H. G. Craighead, P. Neuzil, C. Campagnolo, and C. Batt, *Appl. Phys. Lett.* **77**, 450 (2000).
- [3] H. G. Craighead, *Science* **290**, 1532 (2000).
- [4] K. L. Turner, S. A. Miller, P. G. Hartwell, N. C. MacDonald, S. H. Strogatz, and S. G. Adams, *Nature* (London) **396**, 149 (1998).
- [5] A. H. Nayfeh and D. T. Mook, *Nonlinear Oscillations* (Wiley, New York, 1979).
- [6] M.-F. Yu, M. J. Dyer, G. D. Skidmore, H. W. Rhors, X. K. Lu, K. D. Ausman, J. R. V. Ehr, and R. S. Ruoff, *Nanotechnology* **10**, 244 (1999).
- [7] M. F. Yu, M. J. Dyer, J. Chen, K. Bray, International Conference IEEE-NANO2001, Maui, HI (2001).
- [8] M.-F. Yu, G. J. Wagner, R. S. Ruoff, M. J. Dyer, *Phys. Rev. B* **66**, 073406(2002)
- [9] C. J. Otten, O. R. Lourie, M.-F. Yu, J. M. Cowley, M. J. Dyer, R. S. Ruoff, and W. E. Buhro, *J. Am. Chem. Soc.* **124**, 4564 (2002).
- [10] C. M. Bender and S. A. Orszag, *Advanced Mathematical Methods for Scientists and Engineers* (McGraw-Hill, New York, 1978).